

Time-Resolved Fluorescence Study on the Pressure-Induced Viscosity Dependence of Exciplex Formation in Liquid Solution

Masami Okamoto

Faculty of Engineering and Design, Kyoto Institute of Technology, Matsugasaki, Sakyo-ku, Kyoto 606-8585, Japan

Received: November 5, 1999; In Final Form: February 14, 2000

The contribution of diffusion to the exciplex formation of the 1,2-benzanthracene (BZAN)/dimethylaniline (DMA) and pyrene (PY)/DMA systems in methycyclohexane at pressures up to 400 MPa was investigated. The rate constant, k_3 , for the exciplex formation, which was determined by the analysis of the rise and decay curve of the exciplex emission, decreased significantly with increasing pressure. The apparent activation volume for k_3 , ΔV_3^\ddagger , was 14.9 and 18.1 cm³/mol for BZAN/DMA and PY/DMA, respectively. For comparison, the rate constant, k_q , for the fluorescence quenching by carbon tetrabromide (CBr₄) of BZAN and PY that is believed to be fully diffusion-controlled was also measured as a function of pressure. The apparent activation volume for k_q , ΔV_q^\ddagger , was 17.9 and 20.1 cm³/mol for BZAN/CBr₄ and PY/CBr₄, respectively. These results are interpreted by assuming an encounter complex formed between the donor and acceptor pairs, and it was concluded that the exciplex formation reaction studied in this work is not fully diffusion controlled but competes with a diffusion process of the donor and acceptor molecules that is expressed by a modified Debye equation. It was also concluded that the quenching by CBr₄ is not fully diffusion controlled at the lower pressure range. The bimolecular rate constant, k_{bim} ($= k_c k_{\text{diff}}/k_{-\text{diff}}$), for the exciplex formation was estimated to be $1.5 \times 10^{10} \text{ M}^{-1}\text{s}^{-1}$ for BZAN/DMA and $1.9 \times 10^{10} \text{ M}^{-1}\text{s}^{-1}$ for PY/DMA. The activation volumes for the various rate processes also are discussed.

Introduction

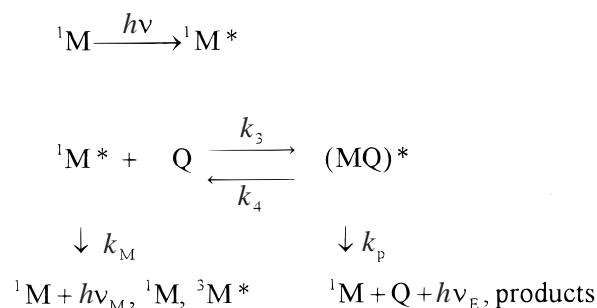
Exciplexes ((MQ)*), which are formed between the lowest electronically excited singlet state (¹M*) and ground state (Q) molecules, have been investigated by many researchers, and the photokinetics is now established.^{1–8} The formation process, k_3 , is often believed to occur with a diffusion-controlled rate for some donor/acceptor systems. When the solute molecules diffuse together in a continuum medium with viscosity, η , the diffusion-controlled rate constant, k_{diff} , is given by

$$k_{\text{diff}} = 8RT/\alpha\eta \quad (1)$$

where α is 3000 and 2000 for the stick and slip boundary limits, respectively, on the basis of the Stokes–Einstein equation.^{9,10} The conclusion that the step of k_3 is diffusion-controlled ($k_3 \sim k_{\text{diff}}$) is mainly due to the $1/\eta$ dependence of k_3 upon changing solvent, temperature,^{1,2,5–8} or pressure.^{11,12} Pollmann and Weller determined the volume change for several exciplex systems in hydrocarbon solvents from the measurements of the fluorescence intensities as a function of pressure by assuming that the step of k_3 is inversely proportional to the pressure-induced solvent viscosity.^{13,14} For radical self-termination reactions¹⁵ and exothermic excitation transfer,^{16,17} which were believed to be diffusion controlled, it has been reported that k_{diff} is not expressed by eq 1 but by a modified equation developed by Spornol and Wirtz.^{18,19} According to this approach, α in eq 1 is replaced by α^{SW} that is related to the properties of solvent and solutes.

Recently, the pressure-induced solvent viscosity dependence of exothermic triplet–triplet excitation transfer was examined in various solvents at pressures up to 400 MPa,²⁰ and the rate

SCHEME 1



constant for diffusion, k_{diff} , was evaluated. It was found that k_{diff} is inversely proportional to the solvent viscosity, and α in eq 1 changes from 2500 to 3590, which is roughly between the stick and slip boundary limits. It was also found that the values of α agree fairly well with those of α^{SW} estimated for the given solutes and solvent system. Based on the evidence, it was concluded that the exothermic energy transfer is not fully diffusion-controlled.

For some exciplex systems, the values of k_3 are significantly smaller than those of k_{diff} predicted by eq 1 ($\alpha = 2000$ or 3000) upon changing temperature and solvent at 0.1 MPa,^{6–8,12} while they seem to approach k_{diff} ($\alpha = 2000$ in eq 1) with increasing pressure when the solvent viscosity is changed by the application of pressure at 25 °C.¹² Such a pressure-induced solvent viscosity dependence is also found for the excimer system.²¹ As a result, the fact that k_3 differs significantly from the k_{diff} predicted by eq 1 implies that the exciplex formation competes with k_{diff} at the lower pressure region as in the case of the exothermic energy transfer.²⁰

TABLE 1: Melting Points, T_{mp} , Boiling Points, T_{bp} , and van der Waals Radii, r_w , of Solutes and Solvent

	T_{mp}/K	T_{bp}/K	r_w/nm^a
1,2-benzanthracene (BZAN)	429	711	0.368
<i>N,N</i> -dimethylaniline (DMA)	276	467	0.314
pyrene (PY)	429	677	0.351
carbon tetrabromide (CBr ₄)	367	463	0.289
methylcyclohexane (MCH)	147	374	0.304

^a Estimated values according to the method of Bondi.²⁹

The present work is focused on the pressure-induced solvent viscosity dependence on k_3 for the typical exciplex systems of pyrene (PY)/*N,N*-dimethylaniline (DMA), and 1,2-benzanthracene (BZAN)/DMA. Therefore, all of the rate constants associated with the exciplex system shown in Scheme 1 were measured in order to obtain further insight of the diffusion-controlled reactions.

Generally, fluorescence is quenched by a heavy-atom perturber. It has been proposed that the quenching occurs via an exciplex between fluorophore and a heavy-atom perturber, the photokinetics of which is similar to Scheme 1, although emission characteristic of the exciplex was not observed.^{22,23} A typical strong quencher, carbon tetrabromide (CBr₄), quenches fluorescence with a diffusion-controlled rate.^{24–28} Therefore, the quenching of fluorescence by CBr₄ of PY and BZAN also was measured as a function of pressure for comparison since k_3 might be expected to involve extra diffusion processes between the donor and acceptor pairs in the solvent cage to form an exciplex as well as their translational diffusion. From the results, together with the data for the pyrene excimer system reported previously,²¹ the contribution of diffusion into k_3 was discussed.

The van der Waals radii of the solute and solvent molecules examined in this work, which are estimated by the method of Bondi,²⁹ together with their melting points and boiling points are listed in Table 1.

Experimental Section

Pyrene (PY) (Wako Pure Chemicals Ltd.) and 1,2-benzanthracene (BZAN) (Tokyo Kasei Organic Chemicals. Co.) of guaranteed grade were chromatographed twice on silica gel (200 mesh), developed and eluted with pentane, and then followed by recrystallization from ethanol. *N,N*-dimethylaniline (DMA) (Wako Pure Chemicals Ltd.) of guaranteed grade was distilled twice under reduced pressure. Methylcyclohexane (MCH) of spectroscopic grade (Dojin Pure Chemicals Co.) was used as received.

Fluorescence decay curve measurements at high pressure were performed by using a 0.3-ns pulse from a PRA LN103 nitrogen laser for excitation. The fluorescence intensity was measured by a Hamamatsu R1635-02 or R928 photomultiplier through a Ritsu MC-25N monochromator, and the resulting signal was digitized by using a Hewlett-Packard 54510A or a Lecroy 9362 digitizing oscilloscope. All data were analyzed by using a NEC PC-9801 or a NEC PC-9821 microcomputer, which was interfaced to the digitizers. The details about the associated high-pressure techniques have been described elsewhere.²⁸

The sample solution was deoxygenated by bubbling nitrogen gas under nitrogen atmosphere for 20 min. The change in the concentration of the quencher by bubbling was corrected by weighing the sample solution. The increase in the concentration due to the application of high pressure was corrected by using the compressibility of the solvent.^{30–32}

TABLE 2: Solvent Viscosity, η , and Rate Constants for BZAN/DMA in MCH

P/MPa	η^a/cP	$k_M^b/10^6 s^{-1}$	$k_3^c/10^9 M^{-1} s^{-1}$	$k_p/10^6 s^{-1}$	$k_4/10^6 s^{-1}$
0.1	0.674	22.9	7.70 ± 0.20	11.9 ± 1.0	144.0 ± 5.0
50	1.143	23.3	5.40 ± 0.26	12.0 ± 1.7	67.0 ± 5.4
100	1.739	23.4	4.24 ± 0.18	11.9 ± 1.5	32.5 ± 4.2
150	2.542	23.6	3.14 ± 0.16	11.8 ± 1.4	17.7 ± 3.8
200	3.752	23.8	2.32 ± 0.08	12.0 ± 1.1	10.4 ± 2.6
250	5.146	23.9	1.72 ± 0.07	11.9 ± 1.0	7.1 ± 2.3
300	7.211	24.0	1.31 ± 0.09	11.9 ± 1.6	5.2 ± 3.0
350	10.02	24.2	1.03 ± 0.08	11.9 ± 1.7	3.9 ± 3.0
400	12.81	24.3	0.74 ± 0.08	12.4 ± 2.2	3.2 ± 3.6

^a References 30–32. ^b Reproducibility was within 1%. ^c Standard deviations estimated from the least-squares slope in the plot of $\lambda_1 + \lambda_2$ against [DMA].

TABLE 3: Rate Constants for PY/DMA in MCH

P/MPa	$k_M^a/10^6 s^{-1}$	$k_3^b/10^9 M^{-1} s^{-1}$	$k_p/10^6 s^{-1}$	$k_4/10^6 s^{-1}$
0.1	2.49	9.45 ± 0.20	9.23 ± 0.47	34.2 ± 4.7
50	2.64	6.04 ± 0.14	9.73 ± 0.48	17.7 ± 1.4
100	2.65	4.18 ± 0.12	10.0 ± 0.06	9.2 ± 2.3
150	2.68	3.18 ± 0.10	9.86 ± 0.56	5.1 ± 1.3
200	2.69	2.38 ± 0.08	10.0 ± 0.58	3.4 ± 1.2
250	2.72	1.76 ± 0.07	10.3 ± 0.65	2.3 ± 1.2
300	2.74	1.36 ± 0.07	10.3 ± 0.76	2.0 ± 1.3
350	2.77	0.99 ± 0.04	10.9 ± 0.55	1.5 ± 1.0
400	2.80	0.75 ± 0.05	11.0 ± 0.81	1.4 ± 1.3

^a Reproducibility was within 1%. ^b Standard deviations estimated from the least-squares slope in the plot of $\lambda_1 + \lambda_2$ against [DMA].

Temperature was controlled at 25 ± 0.2 °C. Pressure was measured by a Minebea STD-5000K strain gauge or a calibrated manganin wire.

Results

Rate Constants for the Exciplex Systems. The fluorescence decay curves in the absence of the quencher exhibit single exponential decays for all of the experimental conditions examined. The values of the decay constant, k_M , are listed in Tables 2 and 3 for BZAN and PY, respectively, and the data of solvent viscosity, η , are also included in Table 2.^{30–32} The values of k_M for pyrene at pressures of up to 300 MPa are in good agreement with those reported previously.²¹

According to Scheme 1, the time dependence of fluorescence intensities for the monomer, $I_M(t)$, and the exciplex, $I_E(t)$, is given for excitation with a pulse of δ -function by^{6,33}

$$I_M(t) = A_1 \exp(-\lambda_1 t) + A_2 \exp(-\lambda_2 t) \quad (2)$$

$$I_E(t) = A_3 \{ \exp(-\lambda_1 t) - \exp(-\lambda_2 t) \} \quad (3)$$

where

$$\lambda_{1,2} = 1/2 [k_M + k_3[Q] + k_4 + k_p \mp \{(k_M + k_3[Q] - k_4 - k_p)^2 + 4k_3k_4[Q]\}^{1/2}] \quad (4)$$

From eq 4, one can obtain

$$\lambda_1 + \lambda_2 = k_M + k_4 + k_p + k_3[Q] \quad (5)$$

$$\lambda_1 \lambda_2 = k_M(k_4 + k_p) + k_3k_p[Q] \quad (6)$$

In the present work, the exciplex emission was used to analyze the rate constants associated with the exciplex formation. The values of λ_1 and λ_2 were determined according to eq 3 by an iterative nonlinear least-squares method with deconvolution. The

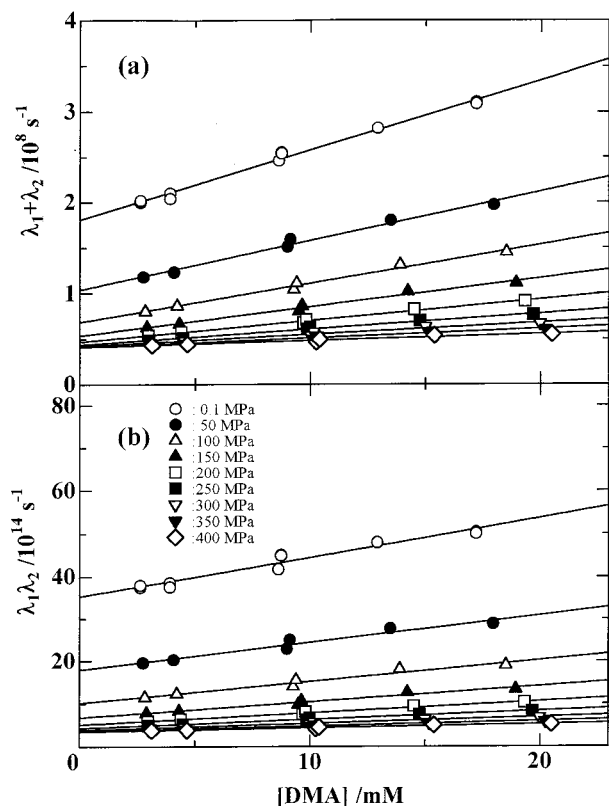


Figure 1. Plots of (a) $\lambda_1 + \lambda_2$ and (b) $\lambda_1\lambda_2$ against [DMA] for BZAN/DMA in MCH at nine different pressures.

plot of $\lambda_1 + \lambda_2$ against $[Q]$ is shown in Figure 1a, and the plot of $\lambda_1\lambda_2$ against $[Q]$ is also shown in Figure 1b for the BZAN/DMA system. As seen in Figure 1, these plots are linear, suggesting that Scheme 1 holds in all of the experimental conditions examined. The values of k_M , k_3 , k_4 , and k_p are listed in Tables 2 and 3 for BZAN/DMA and PY/DMA, respectively, where the values of k_4 determined from eqs 5 and 6 were averaged.

Quenching Constant, k_q , by Carbon Tetrabromide. The fluorescence decay of BZAN and PY in the presence of CBr_4 was measured as a function of the concentration of CBr_4 , $[\text{CBr}_4]$, at pressures of up to 400 MPa, and found to be monoexponential for all of the experimental conditions examined. The quenching rate constant, k_q , was determined by the least-squares slope of the inverse of the lifetime, τ^{-1} , against $[\text{CBr}_4]$, according to

$$1/\tau - 1/\tau_0 = k_q[\text{CBr}_4] \quad (7)$$

where τ_0 is the lifetime in the absence of CBr_4 . Figure 2 shows the plot of $1/\tau$ against $[\text{CBr}_4]$ for BZAN/ CBr_4 . The values of k_q are listed in Table 4 for BZAN/ CBr_4 and PY/ CBr_4 .

Activation Volume. The apparent activation volume, ΔV_i^\ddagger , for the rate constant, k_i , is given by

$$RT(\partial \ln k_i / \partial P)_T = -\Delta V_i^\ddagger \quad (8)$$

The values of ΔV_i^\ddagger for k_i ($i = M, 3, 4$, and p) associated with the exciplex formation at 0.1 MPa are shown in Table 5, together with those for k_q ($i = q$).

Discussion

Contribution of Diffusion to k_3 and k_q . It can be seen in Table 5 that the activation volume, ΔV_i^\ddagger ($i = 3$ and q), is in

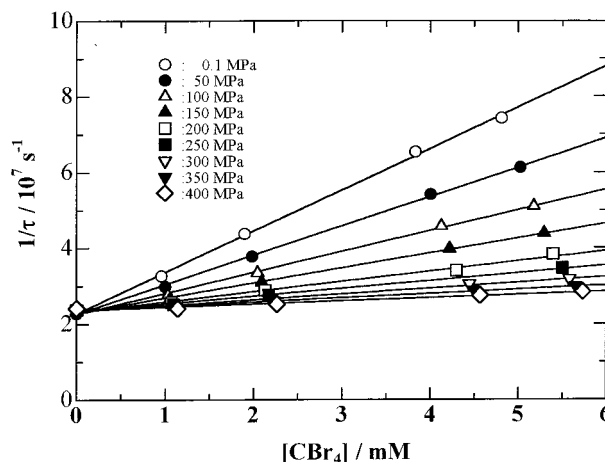


Figure 2. Plots of $1/\tau$ against $[\text{CBr}_4]$ for BZAN/ CBr_4 in MCH at nine different pressures.

TABLE 4: Quenching Rate Constants, k_q , in MCH

P/MPa	$k_q/10^9 \text{ M}^{-1}\text{s}^{-1}$ ^a	
	BZAN/ CBr_4	PY/ CBr_4
0.1	10.8 ± 0.17	11.7 ± 0.50
50	7.71 ± 0.12	7.55 ± 0.21
100	5.48 ± 0.13	5.14 ± 0.11
150	3.90 ± 0.09	3.63 ± 0.08
200	2.66 ± 0.12	2.69 ± 0.08
250	2.00 ± 0.09	2.01 ± 0.07
300	1.50 ± 0.08	1.48 ± 0.05
350	1.09 ± 0.08	1.10 ± 0.05
400	0.81 ± 0.08	0.87 ± 0.03

^a Standard deviations estimated from the least-squares slope in the plot of $1/\tau$ against $[\text{CBr}_4]$.

the range 15–21 cm^3/mol , which is smaller than the activation volume, ΔV_{η}^\ddagger ($24 \pm 1 \text{ cm}^3/\text{mol}$), estimated from the pressure dependence of the solvent viscosity. This suggests that the rate process under consideration is not interpreted simply by a diffusion-controlled reaction. It is noted in Table 5 that ΔV_3^\ddagger for BZAN/DMA is smaller than ΔV_q^\ddagger for BZAN/ CBr_4 , and that ΔV_3^\ddagger for PY/DMA is also smaller than ΔV_q^\ddagger for PY/ CBr_4 . However, at pressures above 300 MPa, ΔV_i^\ddagger ($i = 3$ and q) is roughly equal to ΔV_{η}^\ddagger (ca. 13 cm^3/mol at 350 MPa). The findings, together with the results that k_3 for the exciplex systems is significantly smaller than k_q for BZAN/ CBr_4 and PY/ CBr_4 at lower pressures, imply that k_3 is not fully diffusion controlled.

It has been pointed out by earlier workers that k_{diff} is not correctly described by eq 1.^{9,18,19} In fact, the plot of k_i ($i = 3$ and q) against $1/\eta$ by using data listed in Tables 2–4 showed significant downward curvature. Another test for the diffusion-controlled reaction is the fractional power dependence of η that has been often observed for the nearly or fully diffusion-controlled reaction, given by

$$k_i = A\eta^{\beta_i} \quad (9)$$

where the viscosity exponent, β_i , is normally less than unity.^{34,35} However, as seen in Figure 3, the plot of $\ln k_i$ ($i = 3$ and q) against $\ln \eta$ shows slightly downward curvature although it is almost linear for PY/PY ($\beta_3 = 0.75$).²¹ Such a nonlinear plot of $\ln k_i$ against $\ln \eta$ was found for energy transfer from the triplet state of benzophenone to naphthalene in toluene and the singlet state of triphenylene to benzophenone in *n*-hexane.²⁰ In Figure 3, the mean values of β_i ($i = 3$ and q) are 0.63, 0.86,

TABLE 5: Activation Volumes (cm³/mol) in MCH at 0.1 MPa and 25 °C^a

	ΔV_M^\ddagger	$\Delta V_3^\ddagger/\Delta V_q^\ddagger$	ΔV_4^\ddagger	ΔV_p^\ddagger	ΔV_{-c}^\ddagger
BZAN/DMA	-0.5 ± 0.1	14.9 ± 0.5	40.9 ± 0.6	-0.1 ± 0.1	22.7 ± 1.1
PY/DMA	-1.0 ± 0.2	18.1 ± 0.8	37.7 ± 0.9	-1.0 ± 0.1	22.5 ± 1.5
PY/PY	-1.0 ± 0.5^b	16.8 ± 0.5^c	36^c	-1 ± 1^c	8.1 ± 4.7
BZAN/CBr ₄		17.9 ± 0.5			
PY/CBr ₄		20.1 ± 0.5			

^a ΔV_M^\ddagger for MCH were evaluated to be 24 ± 1 cm³/mol at 25 °C and 0.1 MPa. ^b -2.0 ± 0.5 cm³/mol (reference 21). ^c Reference 21.

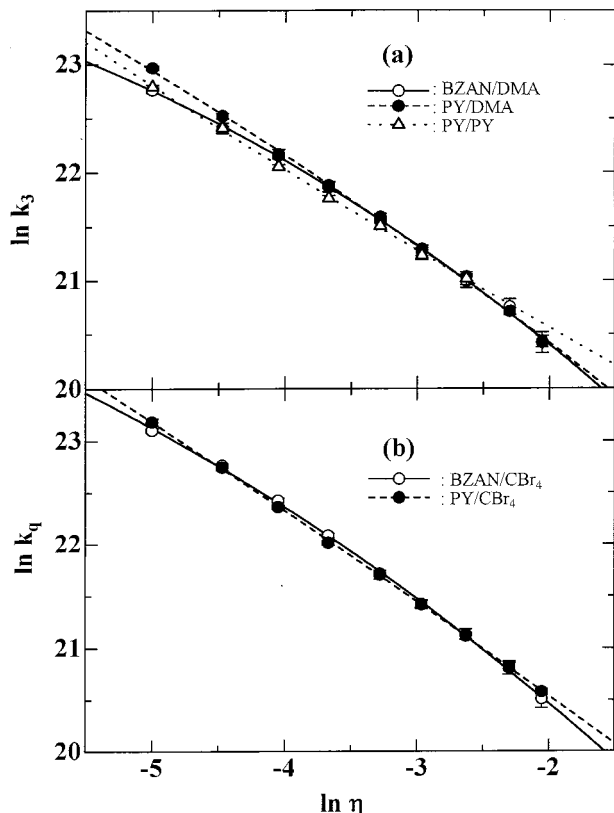
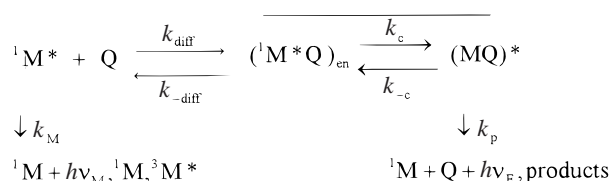


Figure 3. Plots of (a) $\ln k_3$ against $\ln \eta$ for BZAN/DMA, PY/DMA, and PY/PY²¹ and (b) $\ln k_q$ against $\ln \eta$ for BZAN/CBr₄ and PY/CBr₄ in MCH at 25 °C.

SCHEME 2



0.71, and 0.87 for BZAN/DMA, PY/DMA, BZAN/CBr₄, and PY/CBr₄, respectively, at pressures up to 100 MPa and approach to approximately unity at pressures above 300 MPa, being consistent with the discussion of the activation volume described in the previous paragraph. For the heavy-atom quenching systems, the values of β_q are slightly larger than those for the exciplex systems at the low viscosity region, suggesting that the contribution of diffusion to the former systems is larger compared to the latter ones.

In general, exciplex is probably formed via an encounter complex, (${}^1M^*Q$)_{en}, between the donor and acceptor molecules, followed by extra diffusion processes such as a rotational diffusion in a solvent cage (Scheme 2) as for the excimer system,²¹ where the bar indicates the solvent cage, and k_{-diff} is the unimolecular rate constant for dissociation of (${}^1M^*Q$)_{en} in

the solvent cage into ${}^1M^*$ and Q. According to Scheme 2, the observed rate constants of k_3 and k_4 (Scheme 1) are given by

$$k_3 = k_{diff}k_c/(k_{-diff} + k_c) \quad (10)$$

$$k_4 = k_{-diff}k_{-c}/(k_{-diff} + k_c) \quad (11)$$

In eq 10, $k_3 = k_{diff}$ if $k_c \gg k_{-diff}$, and $k_3 = k_{diff}k_c/k_{-diff}$ if $k_{-diff} \gg k_c$: the exciplex formation occurs upon every encounter for the former limiting case, whereas its efficiency is less than unity for the latter case. The fluorescence quenching by CBr₄ may be considered kinetically in the same framework as Scheme 2 in which the step of the dissociation of exciplex, k_4 , is neglected.^{22,23} In this case, the observed quenching rate constant, k_q , is described by the same expression as eq 10.

When the rate constant for diffusion, k_{diff} , is expressed by eq 1, one may derive eq 12 by substituting eq 1 into eq 10

$$\frac{1}{k_3} = \frac{k_{-diff}}{k_{diff}k_c} + \frac{\alpha}{8RT}\eta \quad (12)$$

For the fluorescence quenching by CBr₄, one can obtain a similar relationship to eq 12 in which k_3 is replaced by k_q . The plot of $1/k_3$ against η for BZAN/DMA and PY/DMA is shown in Figure 4a, together with the result for PY/PY reported previously.²¹ It is seen in Figure 4a that the plot is approximately linear with positive intercepts for these three systems. The plot of $1/k_q$ against η for BZAN/CBr₄ and PY/CBr₄, which is shown in Figure 4b, is also linear with a positive intercept. Consequently, the fact that the plot of $1/k_i$ ($i = 3$ or q) against η is linear means that (i) k_{diff} is inversely proportional to the solvent viscosity, η (eq 1) and (ii) the bimolecular rate constant, k_{bim} , defined by $k_{diff}k_c/k_{-diff}$, is apparently independent of pressure (or η), in agreement with the case of the exothermic excitation transfer in solution.²⁰ The values of k_{bim} ($= k_{diff}k_c/k_{-diff}$) and α^{ex} , which were determined from the intercept and slope of the linear plot (Figure 4) by the least-squares method, respectively, are listed in Table 6.

Comparison of α^{ex} with α^{SW} . The value of α^{ex} is very close to the slip boundary limit ($\alpha = 2000$). In a previous publication,²⁰ the solvent viscosity dependence of k_{diff} was discussed on the basis of the Stokes–Einstein equation and an empirical equation proposed by Spornol and Wirtz.^{18,19} For the systems under consideration, α (eq 1) expressed by Spornol and Wirtz, α^{SW} , is given by

$$\alpha^{SW} = \frac{1.2 \times 10^4}{r_{M^*Q}} \left(\frac{1}{f_{M^*}^{SW} r_{M^*}} + \frac{1}{f_Q^{SW} r_Q} \right)^{-1} \quad (13)$$

where r_i is the radius of the spherical solute molecule, i ($i = M^*$ and Q), r_{M^*Q} is the encounter distance, and f_i^{SW} represents a microfriction factor and is given by

$$f_i^{SW} = (0.16 + 0.4r_i/r_s)(0.9 + 0.4T_s^r - 0.25T_i^r) \quad (14)$$

In eq 14, the first parenthetical quantity depends only on the

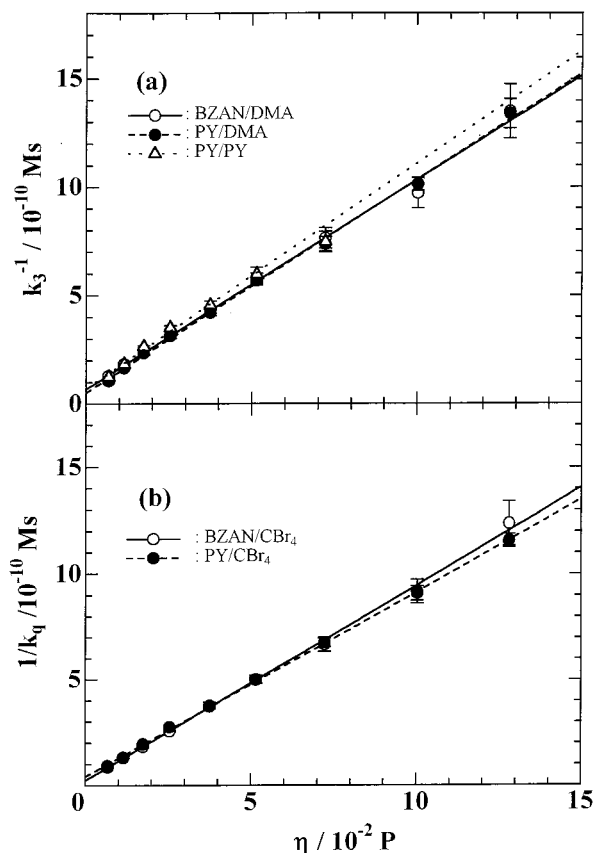


Figure 4. Plots of (a) $1/k_3$ against η for BZAN/DMA, PY/DMA, and PY/PY²¹ and (b) $1/k_q$ against η for BZAN/CBr₄ and PY/CBr₄ in MCH at 25 °C.

TABLE 6: Values of k_{bim} ($= k_{\text{diff}}k_c/k_{\text{-diff}}$) and Those of α^{ex} and α^{SW} in MCH

system	$k_{\text{bim}}/10^{10} \text{ M}^{-1} \text{ s}^{-1}$	α^{ex}	α^{SW^a} trunc/full
BZAN/DMA	1.5 ± 0.3	1920 ± 40	1800/2150
PY/DMA	1.9 ± 0.4	1950 ± 30	1780/2140
PY/PY	1.4 ± 0.2	2060 ± 60	1870/2420
BZAN/CBr ₄	4.6 ± 1.8	1830 ± 30	1720/2270
PY/CBr ₄	2.5 ± 0.3	1740 ± 20	1710/2260

^a Values of $\alpha^{\text{SW}}(\text{trunc})/\alpha^{\text{SW}}(\text{full})$ were estimated by eq 13 (see text).

solute-to-solvent size ratio, (r_i/r_s) (see Table 1). The second parenthetical quantity involves the reduced temperatures, T_s^r and T_i^r , of solvent and solute, respectively, which can be calculated by using the melting point, T_{mp} , and boiling point, T_{bp} , of the solvent or solute at the experimental temperature, T , according to

$$T_{i(S)}^r = [T - T_{\text{mp}(S)}]/[T_{\text{bp}(S)} - T_{\text{mp}(S)}] \quad (15)$$

The values of α^{SW} calculated according to eq 13 at 0.1 MPa are shown in Table 6 in which the α^{SW} (full) and α^{SW} (trunc) were evaluated by eq 14 and by neglecting the second parenthetical quantity in eq 14. We can see in Table 6 that α^{ex} is close to α^{SW} (trunc) and α^{SW} (full).³⁶ This fact may lead to a conclusion that k_{diff} is described satisfactorily by a modified Debye equation (eq 1) for all of the systems examined in this work. Dymond and Woolf³⁷ measured the diffusion coefficient, D , of benzene, toluene, and benzo[*a*]pyrene in hexane at pressures up to 384 MPa and 25 °C. The analysis by using their data revealed that D is approximately inversely proportional to the pressure-induced solvent viscosity, and the values of f_i^{SW} evaluated are in good agreement with those calculated by

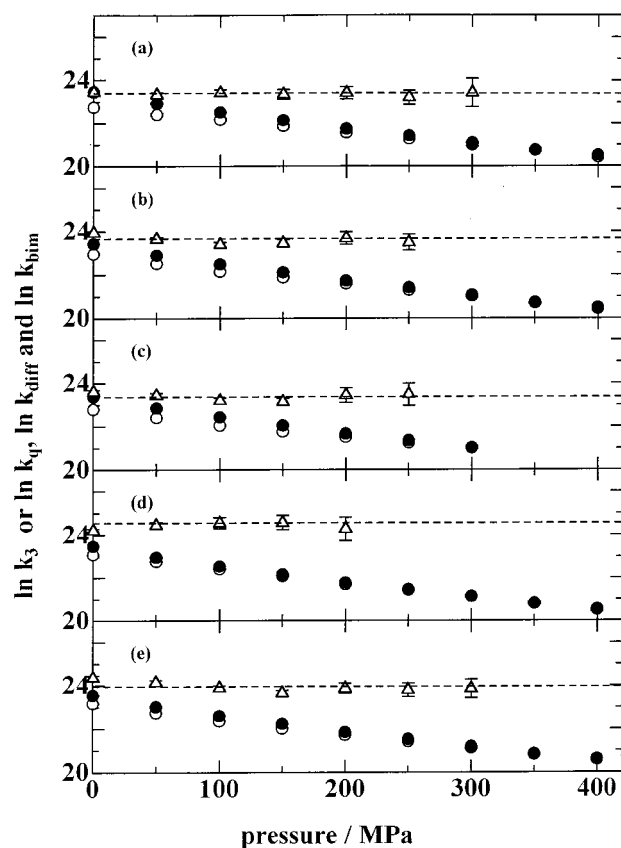


Figure 5. Pressure dependence of k_3 or k_q (O), k_{diff} (●), and k_{bim} (Δ) for BZAN/DMA (a), PY/DMA (b), PY/PY (c), BZAN/CBr₄ (d), and PY/CBr₄ (e) in MCH at 25 °C. The dotted lines represent the values of $\ln k_{\text{bim}}$ determined from the least-squares intercepts of the plots of $1/k_3$ or $1/k_q$ against η (see Table 6).

Spernol and Wirtz.³⁸ The evidence may also support the conclusion mentioned above that k_{diff} is inversely proportional to the pressure-induced solvent viscosity, η (eq 1).

The values of k_{diff} calculated by using α^{ex} and η are shown in Figure 5, together with those of k_i ($i = 3$ or q) for comparison. In Figure 5, k_{diff} decreases from ca. 1.7×10^{10} to $8 \times 10^8 \text{ M}^{-1} \text{ s}^{-1}$ on going from 0.1 to 400 MPa, being almost independent of the systems examined. Furthermore, k_i ($i = 3$ and q) are nearly equal to k_{diff} at pressures above 150 MPa, meaning that the quenching for the systems under consideration is diffusion controlled at the higher pressure region. This is consistent with the observation of the pressure dependence of k_i ($i = 3$ and q) mentioned above.

Bimolecular Rate Constant, $k_{\text{bim}} (= k_c k_{\text{diff}}/k_{\text{-diff}})$. It previously was reported that k_{bim} for exothermic excitation transfer from the triplet states of benzophenone and triphenylene to naphthalene is 1.4 and $1.3 \times 10^{10} \text{ M}^{-1} \text{ s}^{-1}$, respectively, and also that k_{bim} for the singlet state of triphenylene to benzophenone is $3.9 \times 10^{10} \text{ M}^{-1} \text{ s}^{-1}$ in hexane.²⁰ In addition, k_{bim} for energy transfer from the triplet state of 9-acetylanthracene to oxygen was estimated to be $7.1 \times 10^{10} \text{ M}^{-1} \text{ s}^{-1}$ in MCH.³⁵ These values of k_{bim} are compared with those shown in Table 6.

The values of k_{bim} were evaluated by the equation, $k_3 k_{\text{diff}}/(k_{\text{diff}} - k_3)$ or $k_q k_{\text{diff}}/(k_{\text{diff}} - k_q)$ as a function of pressure (see eq 10), and the results are shown in Figure 5, together with those of k_3 or k_q and k_{diff} . We can confirm in Figure 5 that k_{bim} is roughly independent of pressure. The values of k_{bim} for the exciplex and excimer systems are similar in magnitude but are slightly smaller than those for heavy atom quenching systems (Table 6). We also can see in the lower-pressure region that

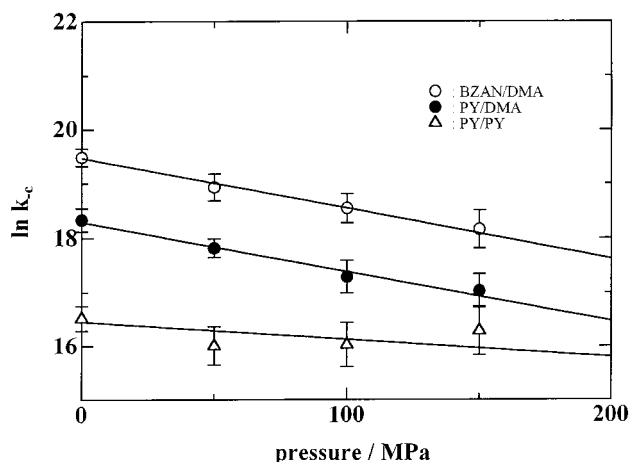


Figure 6. Pressure dependence of k_{-c} for BZAN/DMA, PY/DMA, and PY/PY in MCH at 25 °C.

the difference between k_{bim} and k_{diff} for BZAN/DMA, PY/DMA, and PY/PY is relatively small compared to values observed for the heavy-atom quenching systems, meaning that the contribution of diffusion is significant for the former systems. Thus, the steps for k_3 and k_4 compete with diffusion at the lower-pressure region for all of the systems examined in this work.

Finally, Saltiel et al.^{16,17} have proposed from thermodynamic considerations that $k_{\text{diff}}/k_{-\text{diff}}$ is approximately equal to the inverse of the molarity of the solvent, $1/[S]$, in the study of the exothermic excitation energy transfer at 0.1 MPa. Using this assumption and the data in Table 6, the unimolecular rate constant, k_c , is calculated to be in the range from 1.1×10^{11} (9.1 ps) to $3.6 \times 10^{11} \text{ s}^{-1}$ (2.7 ps) for the systems studied here. The lifetime for intermolecular electron transfer from coumarins to electron-donating solvents such as aniline and DMA, for which no translational diffusion is needed, is in the picosecond time domain.³⁹ This implies that the assumption for $k_{\text{diff}}/k_{-\text{diff}}$ ($= 1/[S]$) by Saltiel et al. is valid to the present systems. However, the pressure dependence of $k_{\text{diff}}/k_{-\text{diff}}$ should be described on the basis of that of the radial distribution function at the closest approach distance of the donor and acceptor pairs in a solvent used,⁴⁰ since the free volume of the system decreases significantly with increasing pressure. In fact, the approach from the radial distribution function in which the solute and solvent molecules are assumed to be hard spheres satisfactorily accounts for the pressure dependence of the quenching of singlet oxygen by the solvent molecules with⁴¹ or without CT interaction,^{42,43} and by the donor molecules^{44–46} in liquid solution. This indicates a moderate increase in $k_{\text{diff}}/k_{-\text{diff}}$ with increasing pressure,⁴⁷ i.e., k_{bim} should increase as pressure increases if k_c is assumed to be independent of pressure. In this case, the plot of $1/k_i$ ($i = 3$ or q) against η is probably still linear with almost identical intercept and slope since k_{bim} increases moderately from the values listed in Table 6, whereas k_{diff} decreases significantly with increasing the solvent viscosity.

Pressure Dependence of k_{-c} . From eqs 10 and 11, together with $k_{\text{bim}} (= k_c k_{\text{diff}}/k_{-\text{diff}})$, the value of k_{-c} can be evaluated by

$$k_{-c} = (k_4/k_3)k_{\text{bim}} \quad (16)$$

The pressure dependence of k_{-c} is shown in Figure 6. The values of k_{-c} are in the range from 1.2×10^7 to $2.9 \times 10^8 \text{ s}^{-1}$ at pressures up to 150 MPa; they are smaller than 1 order of magnitude compared to k_{diff} . This fact suggests that k_{-c} involves a purely chemical activation process. The activation volume, ΔV_{-c}^\ddagger , for the exciplex systems ($i = -c$ in eq 8) is listed in

Table 5, together with that for PY/PY. It is noted in Table 5 that ΔV_{-c}^\ddagger for BZAN/DMA and PY/DMA is significantly larger compared to that for PY/PY. The activation volume, generally, consists of two major contributions, one due to a structure change, $\Delta V_{\text{str}}^\ddagger$, and the other due to a solvation change, $\Delta V_{\text{solv}}^\ddagger$, in activation. Since the charge transfer interaction is relatively small for the excimer systems, ΔV_{-c}^\ddagger for PY/PY may be mainly attributed to the contribution of the structure change in the solvent cage.

For the exciplex systems, ΔV_{-c}^\ddagger may involve the contributions of the loss of solvation ($\Delta V_{\text{solv}}^\ddagger$) as well as a slight increase ($\Delta V_{\text{str}}^\ddagger$) in the distance between M^* and Q of the exciplex, $(MQ)^*$. When the reaction for k_{-c} occurs from an exciplex with dipole moment, μ_e , via a transition state with dipole moment, μ_\ddagger , in continuum medium with dielectric constant, ϵ , the activation volume due to solvation, $\Delta V_{\text{solv}}^\ddagger$, is given by⁴⁸

$$\Delta V_{\text{solv}}^\ddagger = -N_A \left(\frac{\mu_\ddagger^2}{r_\ddagger^3} - \frac{\mu_e^2}{r_e^3} \right) q_p \quad (17)$$

where

$$q_p = \frac{3}{(2\epsilon + 1)^2} \left(\frac{\partial \epsilon}{\partial P} \right)_T$$

In eq 17, r_e and r_\ddagger are the radii for the exciplex and the transition state, respectively, and N_A is Avogadro's number. The largely positive value of ΔV_{-c}^\ddagger for the exciplex systems (Table 5) suggests that the polarity of the transition state for the step of k_{-c} is less than that of the exciplex, $(MQ)^*$. We assume that $\mu_\ddagger \sim 0$ in order to estimate the maximum volume of activation for the loss of solvation. The values of $N_A \mu_e / r_e^3$ in eq 17 have been measured for several donor and acceptor pairs from the solvent dependence of the emission band maximum; they are 6.2×10^4 and $6.6 \times 10^4 \text{ cm}^3 \text{ MPa mol}^{-1}$ for PY/DMA⁴⁹ and PY/*N,N*-diethylaniline,⁵⁰ respectively, and $5.9 \times 10^4 \text{ cm}^3 \text{ MPa mol}^{-1}$ for BZAN/*N,N*-diethylaniline.^{14,50} From these values, together with the known value of q_p for MCH ($1.847 \times 10^{-4} \text{ MPa}^{-1}$),⁵¹ the maximum value of $\Delta V_{\text{solv}}^\ddagger$ can be estimated to be $11.4 \text{ cm}^3/\text{mol}$ for PY/DMA and $10.9 \text{ cm}^3/\text{mol}$ for BZAN/*N,N*-diethylaniline. The value for the latter system may be nearly equal to that for BZAN/DMA, judging from the fact that the difference in $N_A \mu_e / r_e^3$ for PY/DMA and PY/*N,N*-diethylaniline is not significant. Therefore, $\Delta V_{\text{str}}^\ddagger$ due to the structure change for both the exciplex systems in the solvent cage is calculated to be ca. $10 \text{ cm}^3/\text{mol}$, nearly equal to $\Delta V_{\text{str}}^\ddagger$ for PY/PY.

Summary

It has been demonstrated from the high-pressure study that the processes of exciplex formation for BZAN/DMA and PY/DMA and also for the fluorescence quenching by CBr₄ of BZAN and PY are not fully diffusion controlled in methylcyclohexane but compete with a diffusion process that is expressed by a modified Debye equation (eq 1). The bimolecular rate constant, k_{bim} , defined by $k_{\text{diff}}k_c/k_{-\text{diff}}$, has been found to be approximately constant in MCH at pressures up to 400 MPa. It is noted that the nonlinear plot between $\ln k_q$ and $\ln \eta$ and also the linear plot between $\ln k_q$ and $\ln \eta$ with the slope larger than -1 are due to the contribution of bimolecular rate processes to the diffusion, in agreement with the conclusion reported previously.²⁰

Finally, as mentioned briefly in the last paragraph of the section of bimolecular rate constants, it is important to obtain the experimental evidence about the pressure dependence of $k_{\text{diff}}/$

$k_{\text{-diff}}$ that is most likely described by the radial distribution function at contact of the donor and acceptor pairs in liquid solution. Based on this theory, $k_{\text{diff}}/k_{\text{-diff}}$ should increase moderately with increasing pressure.⁴⁰ The quenching system with lower k_{bim} compared to k_{diff} may give insight into this problem.⁵²

Acknowledgment. This work was partly supported by a Grant-in-Aid for Scientific Research from the Ministry of Education of Japan (No. 06640651).

References and Notes

- (1) Ware, W. R.; Richter, H. P. *J. Chem. Phys.* **1968**, *48*, 1595.
- (2) Yoshihara, K.; Kasuya, T.; Inoue, A.; Nagakura, S. *Chem. Phys. Lett.* **1971**, *9*, 469.
- (3) Nakashima, N.; Mataga, N. *Z. Phys. Chem.* **1972**, *79*, 150.
- (4) Nakashima, N.; Mataga, N.; Yamanaka, C. *Int. J. Kinet.* **1973**, *5*, 833.
- (5) Ware, W. R.; Watt, D.; Holmes, J. D. *J. Am. Chem. Soc.* **1974**, *96*, 7853.
- (6) Hui, M. H.; Ware, W. R. *J. Am. Chem. Soc.* **1976**, *98*, 4712, 4718.
- (7) O'Connor, D. V.; Ware, W. R. *J. Am. Chem. Soc.* **1979**, *101*, 121.
- (8) Cheung, S. T.; Ware, W. R. *J. Phys. Chem.* **1983**, *87*, 466.
- (9) Birks, J. B. *Organic Molecular Photophysics*; Wiley: New York, 1973; p 403.
- (10) Rice, S. A. In *Comprehensive Chemical Kinetics. Diffusion-Limited Reactions*; Bamford, C. H., Tripper, C. F. H., Compton, R. G., Eds; Elsevier: Amsterdam, 1985; Vol. 25.
- (11) Turely, W. R.; Offen, H. W. *J. Phys. Chem.* **1984**, *88*, 3605.
- (12) Okamoto, M.; Tanaka, F.; Teranishi, H. *J. Phys. Chem.* **1986**, *90*, 1055.
- (13) Pollmann, P.; Weller, A. *Ber. Bunsen-Ges. Phys. Chem.* **1973**, *77*, 10716.
- (14) Pollmann, P.; Weller, A. *Ber. Bunsen-Ges. Phys. Chem.* **1975**, *79*, 692.
- (15) Schuh, H.-H.; Fischer, H. *Helv. Chim. Acta* **1978**, *61*, 2130.
- (16) Saltiel, J.; Shannon, P. T.; Zafiriou, O. C.; Uriarte, K. *J. Am. Chem. Soc.* **1980**, *102*, 6799.
- (17) Saltiel, J.; Atwater, B. W. *Advances in Photochemistry*; Wiley-Interscience: New York, 1987; Vol. 14, p 1.
- (18) Spornol, A.; Wirtz, K. *Z. Naturf.* **1953**, *8A*, 522.
- (19) Gierer, A.; Wirtz, K. *Z. Naturf.* **1953**, *8A*, 532.
- (20) Okamoto, M. *J. Phys. Chem. A* **1998**, *102*, 4751.
- (21) Okamoto, M.; Sasaki, M. *J. Phys. Chem.* **1991**, *95*, 6548.
- (22) Birks, J. B. *Photophysics of Aromatic Molecules*; Wiley-Interscience: New York, 1970; p 443.
- (23) Shimizu, Y.; Azumi, T. *J. Phys. Chem.* **1982**, *86*, 22.
- (24) Bowen, E. J.; Metcalf, W. S. *Proc. R. Soc. A* **1951**, *206*, 437.
- (25) Melhuish, H. W.; Metcalf, W. S. *J. Chem. Soc.* **1954**, 976. Melhuish, H. W.; Metcalf, W. S. *J. Chem. Soc.* **1958**, 480.
- (26) Ware, W. R.; Novros, J. S. *J. Phys. Chem.* **1966**, *70*, 3246.
- (27) Nemzek, T. M.; Ware, W. R. *J. Chem. Phys.* **1975**, *62*, 477.
- (28) Okamoto, M.; Teranishi, H. *J. Phys. Chem.* **1984**, *88*, 5644.
- (29) Bondi, A. *J. Phys. Chem.* **1964**, *68*, 441.
- (30) Bridgman, P. W. *Proc. Am. Acad. Arts Sci.* **1926**, *61*, 57.
- (31) Brazier, D. W.; Freeman, G. R. *Can. J. Chem.* **1969**, *47*, 893.
- (32) Jonas, J.; Hasha, D.; Huang, S. G. *J. Chem. Phys.* **1979**, *71*, 15.
- (33) Birks, J. B. *Organic Molecular Photophysics*; Wiley: New York, 1973; p 84.
- (34) Hirayama, S.; Yasuda, H.; Scully, A. D.; Okamoto, M. *J. Phys. Chem.* **1994**, *98*, 4609, and references therein.
- (35) Okamoto, M.; Tanaka, F.; Hirayama, S. *J. Phys. Chem. A* **1998**, *102*, 10703.
- (36) The values of $f_i^{\text{SW}}(\text{full})$ were calculated to be 0.826, 0.808, 0.651, and 0.727, and those of $f_i^{\text{SW}}(\text{trunc})$ 0.644, 0.622, 0.573, and 0.541 for BZAN, PY, DMA, and CBr₄, respectively. According to the Stokes-Einstein equation, the diffusion coefficient of a spherical solute molecule, i , with the radius, r_i , D_i^{SE} , is given by $D_i^{\text{SE}} = k_B T / f_i^{\text{SE}} \pi \eta r_i$, where $f_i = 6$ and 4 for the stick and slip boundary limits, respectively. Spornol and Wirtz^{18,19} introduced a microfriction factor, f_i^{SW} , and described the diffusion coefficient, D_i^{SW} , as $D_i^{\text{SW}} = k_B T / 6 \pi f_i^{\text{SW}} \eta r_i$. Therefore, $f_i^{\text{SW}} = 1$ and 2/3 for the stick and slip boundary limits, respectively.
- (37) Dymond, J. H.; Woolf, L. A. *J. Chem. Soc., Faraday Trans. 1* **1982**, *78*, 991.
- (38) The values of f_i^{SW} determined from the least-squares slopes of the plots of D against $1/\eta$ in hexane at 25 °C were 0.50 ± 0.02 , 0.51 ± 0.02 , and 0.65 ± 0.02 for benzene, toluene, and benzo[*a*]pyrene, respectively, since the radii of the solute and solvent molecules can be evaluated by the method of Bondi.²⁹ The values of $f_i^{\text{SW}}(\text{trunc})/f_i^{\text{SW}}(\text{full})$ calculated were 0.52/0.56, 0.54/0.55, and 0.65/0.84 for benzene, toluene, and benzo[*a*]pyrene, respectively.
- (39) Yoshihara, K. *Advances in Chemical Physics*; Wiley: New York, 1999; Vol. 107, p 371, and references therein.
- (40) Yoshimura, Y.; Nakahara, M. *J. Chem. Phys.* **1984**, *81*, 4080.
- (41) Okamoto, M.; Tanaka, F. *J. Phys. Chem.* **1993**, *97*, 177.
- (42) Okamoto, M.; Tanaka, F.; Teranishi, H. *J. Phys. Chem.* **1990**, *94*, 669.
- (43) Schmidt, R.; Seikel, K.; Brauer, H.-D. *Ber. Bunsen-Ges. Phys. Chem.* **1990**, *94*, 1100.
- (44) Seikel, K.; H.-D. Brauer, H.-D. *Ber. Bunsen-Ges. Phys. Chem.* **1991**, *95*, 900.
- (45) Hild, M.; Brauer, H.-D. *Ber. Bunsen-Ges. Phys. Chem.* **1996**, *100*, 1210.
- (46) Okamoto, M. *J. Photochem. Photobiol. A Chem.* **1999**, *124*, 113.
- (47) The values of $\Delta V_{\text{diff}}^{\ddagger} - \Delta V_{-\text{diff}}^{\ddagger}$ were calculated to be -10.5, -10.5, -10.6, -10.4, and -10.4 cm³/mol at 0.1 MPa for BZAN/DMA, PY/DMA, PY/PY, BZAN/CBr₄, and PY/CBr₄, respectively; the values of the hard-sphere radii listed in Table 1 were used for the calculation of the radial distribution function at the closest approach distance,⁴⁰ and the value of $RT\kappa$ of 2.5 cm³,³⁰⁻³² where κ is the isothermal compressibility of the solvent at 25 °C and 0.1 MPa, was used for the calculation of $\Delta V_{\text{diff}}^{\ddagger} - \Delta V_{-\text{diff}}^{\ddagger}$.⁴⁰
- (48) Kirkwood, J. G. *J. Chem. Phys.* **1934**, *2*, 351.
- (49) Mataga, N.; Okada, T.; Yamamoto, N. *Bull. Chem. Soc. Jpn.* **1966**, *39*, 2562.
- (50) Beens, H.; Knibbe, H.; Weller, A. *J. Chem. Phys.* **1967**, *47*, 1183.
- (51) Hartmann, H.; Newmann, A.; Schmidt, A. P. *Ber. Bunsen-Ges. Phys. Chem.* **1968**, *72*, 877.
- (52) Okamoto, M., to be submitted.